The geomagnetic power spectrum

Stefan Maus

CIRES, University of Colorado, and NOAA's National Geophysical Data Center. E-mail: Stefan.maus@noaa.gov

SUMMARY

Combining CHAMP satellite magnetic measurements with aeromagnetic and marine magnetic data, the global geomagnetic field has now been modelled to spherical harmonic degree 720. An important tool in field modelling is the geomagnetic power spectrum. It allows the comparison of field models estimated from different data sets and can be used to identify noise levels and systematic errors. A correctly defined geomagnetic power spectrum is flat (white) for an uncorrelated field, such as the Earth's crustal magnetic field at long wavelengths. It can be inferred from global spherical harmonic models as well as from regional grids. Marine and aeromagnetic grids usually represent the anomaly of the total intensity of the magnetic field. Appropriate corrections have to be applied in estimating the geomagnetic power spectrum from such data. The comparison of global and regional spectra using a consistently defined azimuthally averaged geomagnetic power spectrum facilitates quality control in field modelling and should provide new insights in magnetic anomaly interpretation.

Key words: Spatial analysis; Magnetic anomalies: modelling and interpretation; Satellite magnetics.

INTRODUCTION

A new generation of low-orbiting magnetic field satellites provides increasingly accurate measurements of the Earth's magnetic field. With the slowly decreasing altitude of the CHAMP satellite under solar minimum conditions, the MF series of CHAMP crustal magnetic field models was gradually extended to spherical harmonic degree 100 for the latest MF5 model (Maus *et al.* 2007a). A significantly higher degree model was produced by combining MF5 with the aeromagnetic and marine magnetic data holdings of the National Geophysical Data Center (NGDC). In 2006 September, the NGDC-720 model to SH degree 720 was released and made available online at http://ngdc.noaa.gov/seg/EMM/emm.shtml as SH coefficients and software. Marine and aeromagnetic data have also been directly compiled into World Magnetic Anomaly Maps (Hamoudi *et al.* 2007; Hemant *et al.* 2007; Maus *et al.* 2007b). Their grids have 3 arcmin resolution but are not available as spherical harmonic expansions of the magnetic potential.

An interesting characteristic of the geomagnetic field is its variance as a function of spherical harmonic degree. As demonstrated by Mauersberger (1956) and Lowes (1966), the total variance R of the magnetic field can be broken up into a sum of individual contributions R_ℓ of different SH degree ℓ, given by

$$R_\ell = (\ell + 1) \left(\frac{R_e}{r} \right)^{2\ell+4} \sum_{m=-\ell}^{\ell} \left(g_\ell^m \right)^2, \qquad (1)$$

where $R_e = 6371.2$ is the geomagnetic reference radius and g_ℓ^m are the Gauss coefficients of the field. The degree variance, sometimes called Mauersberger–Lowes spectrum, is shown in Fig. 1 for some recent field models. Using degree variances inferred from a

Magsat field model, Langel & Estes (1982) discovered the 'knee' at degree 15, separating the main magnetic field at low degrees from the crustal magnetic field at high degrees. The characteristics of core and crustal field variances of Earth and Mars were recently summarized by Voorhies *et al.* (2002). Degree variances of the Earth's crustal magnetic field have also been predicted from statistical models of the crustal magnetization (Jackson 1996; McLeod 1996). McLeod & Coleman (1980) derived the average power spectra of magnetic field vector components on great circles from the spherical harmonic coefficients of the magnetic potential. O'Brien *et al.* (1999) inverted these relations to estimate global degree variances from vector component aeromagnetic survey lines over the oceans.

With a new generation of highly accurate satellite magnetic measurements, it has become increasingly clear that the degree variance shows an awkward upward slope of the crustal field towards higher degrees. If interpreted as a power spectrum, this would suggest that geomagnetic field models were strongly contaminated by noise. However, the degree variance is not a power spectrum in the usual sense. As pointed out by Hipkin (2001), the degree variance slopes upward for a spatially uncorrelated field. Interpreting degree variances as a spatial power spectrum (e.g. Lowes 1974) can, therefore, lead to serious misinterpretation. As shown here, a correctly defined geomagnetic power spectrum is flat for the long wavelength crustal field. Conversely, the fact that the degree variance is almost flat at the core–mantle boundary does not mean that the field is spatially uncorrelated there.

Prior to the CHAMP satellite mission, a large spectral gap existed between global satellite-based field models and regional magnetic anomaly maps. Using degree variances as power spectra did not create obvious problems. However with a closing spectral gap, it is
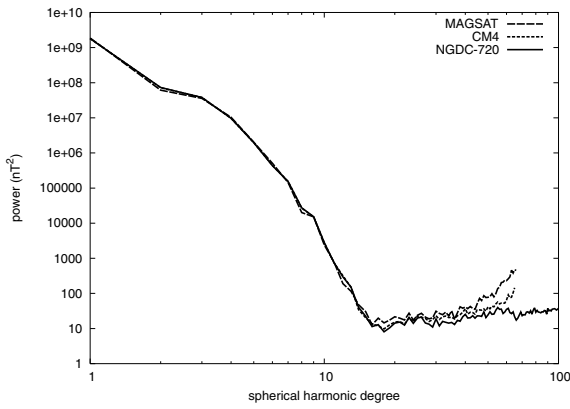
Figure 1. Degree variances of some recent geomagnetic field models (Cain *et al.* 1989; Sabaka *et al.* 2004). The upward slope above degree 15 should not be interpreted as a noise contamination because the degree variance slopes upward for a spatially uncorrelated field. A correctly defined geomagnetic power spectrum has a flat crustal field spectrum (see Fig. 4).

important to have compatible definitions of the geomagnetic power spectrum for global and regional data sets. Here, I provide a complete derivation of the geomagnetic power spectrum for spherical harmonic expansions and plane grids. This yields the appropriate scaling factors, including multiples of the Earth radius R_e, grid side length L and number of grid cells n, to bring spherical and plane spectra to a common power level. A complication arises because regional grids usually represent the anomaly of the total intensity rather than the vector of the magnetic field. While the total intensity measurements do not completely determine the field vector, it is shown here that the magnetic field spectrum can nevertheless be estimated from such data. The usefulness of the new definitions is demonstrated by comparing the global NGDC-720 spectrum with the average corresponding spectra of local subgrids from NGDC's World Magnetic Anomaly Map (Maus *et al.* 2007b).

THEORY

The main challenge in defining a geomagnetic power spectrum is to find the correct scale factors. The idea behind the following derivation is to first define the power in a coordinate-independent way, and then decompose it into contributions from different wavelengths for a specific coordinate system.

The internal magnetic field **B** on the surface of the Earth has an expected value $E\{\mathbf{B}(x_1, x_2)\}$ at the location (x_1, x_2) and a variance

$$E\left\{[\mathbf{B}(x_1, x_2) - E\{\mathbf{B}(x_1, x_2)\}]^2\right\} = E\left\{\mathbf{B}(x_1, x_2)^2\right\} - E\{\mathbf{B}(x_1, x_2)\}^2,$$
(2)

where all squares and multiplications of vectors are to be read as scalar products. The quantity $E\{\mathbf{B}(x_1, x_2)^2\}$ shall be referred to as the power of the field. This power can be written as an integral over the 2-D spectral density $P(k_1, k_2)$ as

$$E\{\mathbf{B}(x_1, x_2)^2\} = \int_{-\infty}^{\infty} \int_{-\infty}^{\infty} P(k_1, k_2) \, dk_1 \, dk_2$$
(3)

$$= \int_{0}^{\infty} \int_{0}^{2\pi} P(k \cos\alpha, k \sin\alpha) \, k \, d\alpha \, dk,$$
(4)

where $k = \sqrt{k_1^2 + k_2^2}$ is the wavenumber measured in radians per kilometre, and α is the azimuth. In contrast to the wavenumber, the azimuth depends on the orientation of the coordinate system.

There are several possibilities to define a spectral density $P(k)$ which is only a function of the wavenumber and independent of the azimuth. However, to avoid misinterpretation, $P(k)$ should be defined in such a way that it is flat for a spatially uncorrelated 'white noise' magnetic field $\mathbf{W}(x_1, x_2)$.

The autocorrelation function of a white noise magnetic field $\mathbf{W}(x_1, x_2)$ is a Dirac δ-function. Its 2-D spectral density $P(k_1, k_2)$, which is the 2-D Fourier transform of the autocorrelation function, is constant. We therefore, have the simple situation in which the 1-D spectral density of any cross-section of $\mathbf{W}(x_1, x_2)$ is constant, and the 2-D spectral density $P(k_1, k_2)$ is also constant. The desired spectral density $P(k)$ is also constant if it is not defined as an azimuthal sum but as an azimuthal average of $P(k_1, k_2)$ as in

$$P(k) = \frac{1}{2\pi} \int_{0}^{2\pi} P(k \cos\alpha, k \sin\alpha) \, d\alpha.$$
(5)

With definition (5) the expected power in eq. (4) can be written as

$$E\{\mathbf{B}(x_1, x_2)^2\} = \int_{0}^{\infty} P(k) \, 2\pi k \, dk.$$
(6)

Values of $P(k)$ carry the unit $nT^2 \, km^2$, which is the unit of a 2-D power spectral density. The spectral density $P(k)$ as defined in (5) is independent of the coordinate-system.

Spherical harmonic power spectrum

In geocentric spherical polar coordinates, with radius r, colatitude ϑ and longitude φ, we can write **B**, following the notation of Backus *et al.* (1996), as a sum of spherical harmonic contributions $\mathbf{B}_\ell^m$ of degree ℓ and order m as

$$\mathbf{B}(\vartheta, \varphi) = \sum_{\ell=1}^{\infty} \sum_{m=-\ell}^{\ell} \mathbf{B}_\ell^m(\vartheta, \varphi),$$
(7)

where increasing values of ℓ on a sphere with radius r correspond to decreasing wavelengths $\lambda = 2\pi r/(\ell + 1/2)$. The contributions are orthogonal in the sense that

$$\langle \mathbf{B}_\ell^m(\vartheta, \varphi) \mathbf{B}_{\ell'}^{m'}(\vartheta, \varphi) \rangle = 0 \text{ for } \ell \neq \ell' \text{ or } m \neq m',$$
(8)

where $\langle \cdot \rangle$ denotes the mean over the surface of the sphere. Then the power can be written as

$$E\{\mathbf{B}(\vartheta, \varphi)^2\} = \langle \mathbf{B}(\vartheta, \varphi)^2 \rangle = \sum_{\ell=1}^{\infty} \sum_{m=-\ell}^{\ell} \langle \mathbf{B}_\ell^m(\vartheta, \varphi)^2 \rangle$$
(9)

defining a discrete representation of the power in terms of contributions of degree ℓ and order m. Let us now represent the magnetic field contribution $\mathbf{B}_\ell^m$ in the usual way as the gradient of a scalar magnetic potential ψ:

$$\mathbf{B}_\ell^m = -\nabla \psi_\ell^m = -\left(\frac{1}{r}\nabla_s + \hat{\mathbf{r}}\partial_r\right)\psi_\ell^m,$$
(10)

with surface gradient $\nabla_s = r\nabla - \mathbf{r}\partial_r = \hat{\boldsymbol{\vartheta}}\partial_\vartheta + (\hat{\boldsymbol{\varphi}}/\sin\vartheta)\partial_\varphi$. The magnetic potential is given in terms of the Gauss coefficients g_ℓ^m as

$$\psi_\ell^m(r, \vartheta, \varphi) = R_e \left(\frac{R_e}{r}\right)^{\ell+1} g_\ell^m \, \beta_\ell^m(\vartheta, \varphi),$$
(11)

where the Schmidt semi-normalized spherical harmonic basis functions $\beta_\ell^m(\vartheta, \varphi)$ (Backus *et al.* 1996, p. 141–142) are defined as

$$\beta_\ell^m = \cos m\varphi \, \breve{P}_\ell^m(\cos\vartheta), \quad 0 \leq m \leq \ell$$
(12)

$$\beta_\ell^{-m} = \sin m\varphi \; \check{P}_\ell^m(\cos\vartheta), \quad 1 \le m \le \ell, \tag{13}$$

and the functions $\check{P}_\ell^m(\mu)$ are given by

$$\check{P}_\ell^m(\mu) = \begin{cases} \sqrt{2\frac{(\ell-m)!}{(\ell+m)!}} \, P_\ell^m(\mu) & \text{if } 1 \le m \le \ell \\ P_\ell(\mu) & \text{if } m = 0, \end{cases} \tag{14}$$

where $P_\ell^m(\mu)$ are the associated Legendre functions (eq. 3.7.2 Backus *et al.* 1996). Then the power at a particular degree and order can be written (Backus *et al.* 1996, p. 145–146) as

$$\left\langle \left(\mathbf{B}_\ell^m \right)^2 \right\rangle = \left\langle \left(\frac{1}{r} \nabla_s \psi_\ell^m \right)^2 \right\rangle + \left\langle (\hat{\mathbf{r}}\partial_r) \psi_\ell^m)^2 \right\rangle \tag{15}$$

$$= (g_\ell^m)^2 \left(\frac{R_e}{r} \right)^{2\ell+4} \left[\left\langle (\nabla_s \beta_\ell^m)^2 \right\rangle + \left\langle (\ell+1)^2 (\beta_\ell^m)^2 \right\rangle \right] \tag{16}$$

$$= (g_\ell^m)^2 \left(\frac{R_e}{r} \right)^{2\ell+4} \frac{\ell(\ell+1) + (\ell+1)^2}{2\ell+1} \tag{17}$$

$$= (\ell+1)(g_\ell^m)^2 \left(\frac{R_e}{r} \right)^{2\ell+4}. \tag{18}$$

The discrete representation of the geomagnetic field power (9) then becomes

$$E\{\mathbf{B}(\vartheta,\varphi)^2\} = \sum_{\ell=1}^{\infty} (\ell+1) \left(\frac{R_e}{r} \right)^{2\ell+4} \sum_{m=-\ell}^{\ell} (g_\ell^m)^2. \tag{19}$$

In (19) a sum over the index m is followed by an outer sum over the harmonic degree ℓ. In contrast to ℓ, the azimuthal index m depends on the orientation of the coordinate system. As in definition (5), we become independent of the coordinate system by averaging over the azimuthal index m. Performing the inner azimuthal sum in (19) then gives

$$E\{\mathbf{B}(\vartheta,\varphi)^2\} = \sum_{\ell=1}^{\infty} (2\ell+1) S_\ell, \tag{20}$$

where the geomagnetic power spectrum S_ℓ is defined as

$$S_\ell = \frac{\ell+1}{2\ell+1} \left(\frac{R_e}{r} \right)^{2\ell+4} \sum_{m=-\ell}^{\ell} (g_\ell^m)^2. \tag{21}$$

This is the definition that should be used for the geomagnetic power spectrum instead of R_ℓ of eq. (1). The quantity S_ℓ of eq. (21) provides the average power per independent mode, of which there are $2\ell+1$ for each degree ℓ. This is consistent with the usual definition of a spatial power spectrum. In contrast, R_ℓ provides the total power of all modes combined for a given degree. As pointed out by Hipkin (2001), the quantity R_ℓ is, therefore, more adequately referred to as the degree variance, rather than a power spectrum. The degree variance, computed as an azimuthal sum (rather than an average) over the orders m, slopes upward with increasing degree ℓ for a spatially uncorrelated field, as seen for the Earth's crustal magnetic field at long wavelengths (Fig. 1).

In order to establish compatibility with plane grids, we have to extend the discrete geomagnetic power spectrum (21) into a continuous spectral density. Extending the discrete function S_ℓ into a continuous step function $S(\ell)$, where $S(\ell) = S_{\text{round}(\ell)}$, we can write eq. (20) as

$$E\{\mathbf{B}(\vartheta,\varphi)^2\} = \int_{1/2}^{\infty} (2\ell+1) S(\ell) \, d\ell. \tag{22}$$

Integration starts at 1/2, as the lowest value that will round to $\ell = 1$. Next, let us transform the integrand to a function of the wavenumber k. The wavenumber of a spherical harmonic of degree ℓ is (p. 103 Backus *et al.* 1996)

$$k = \frac{\sqrt{\ell(\ell+1)}}{r} \approx \frac{\ell+1/2}{r}. \tag{23}$$

We can substitute $d\ell = r \, dk$, giving

$$E\{\mathbf{B}(\vartheta,\varphi)^2\} = \int_{1/r}^{\infty} 2rk \; S(rk - 1/2) \, r \, dk \tag{24}$$

$$= \int_{1/r}^{\infty} \underbrace{\frac{r^2 \; S(rk-1/2)}{\pi}}_{P(k)} 2\pi k \, dk \tag{25}$$

Hence, the expected power $E\{\mathbf{B}(\vartheta,\varphi)^2\}$ can be written as an integral over the spectral density $P(k)$, as prescribed in the normalization condition (6). The spherical harmonic coefficients g_ℓ^m provide values of $P(k)$ at wavenumbers $k_\ell = (\ell+1/2)/r$ with

$$P(k_\ell) = \frac{r^2 S(\ell)}{\pi} = \frac{r^2(\ell+1)}{\pi(2\ell+1)} \left(\frac{R_e}{r} \right)^{2\ell+4} \sum_{m=-\ell}^{\ell} (g_\ell^m)^2. \tag{26}$$

This spectral density $P(k_\ell)$ follows from the discrete geomagnetic power spectrum (21) by multiplication with r^2/π. The spectral density $P(k)$ is used later to relate plane spectra to the geomagnetic power spectrum S_ℓ. It is also useful for comparing magnetic field spectra from different planets because, in contrast to S_ℓ of (21), the spectral density $P(k)$ of (26) is an absolute measure of field variability, independent of the radius of the sphere on which the data are collected. For example, if $_E g_\ell^m$ and $_M g_\ell^m$ are the Gauss coefficients of the terrestrial and martian magnetic fields, respectively, then $P(k)$ of (26) allows for the direct comparison of magnetic field power spectra for Earth and Mars. This compatibility follows directly from definitions (4) to (6), but it is not easy to see in (26) because the Gauss coefficients g_ℓ^m depend on the chosen planetary reference radius R_e.

Total intensity spectrum

Aeromagnetic surveys usually resolve only the total intensity of the field. This is primarily due to the technical difficulty of accurately orienting a vector magnetometer on an aircraft. To compare such data with global field models, one can estimate the total intensity spectrum from the aeromagnetic data and compare it with the global total intensity spectrum. A more attractive possibility, discussed below, is to directly estimate the geomagnetic power spectrum corresponding to eq. (21) from the local total intensity data.

There are two ways of obtaining a globally averaged total intensity spectrum from the spherical harmonic coefficients of the magnetic potential. A numerical approach is to use a reverse spherical harmonic transform to compute a latitude/longitude grid of the magnetic field $\mathbf{B}$ from the Gauss coefficients g_ℓ^m. Then compute $|\mathbf{B}|$ and obtain the spherical harmonic coefficients of $|\mathbf{B}|$ by a forward transform. These coefficients can then be used to compute the exact total intensity spectrum T_ℓ by

$$T_\ell = \frac{1}{(2\ell+1)^2} \sum_{m=-\ell}^{\ell} (t_\ell^m)^2, \tag{27}$$

where t_ℓ^m are the Schmidt semi-normalized spherical harmonic coefficients of the total intensity. Here, one division by $(2\ell+1)$ is
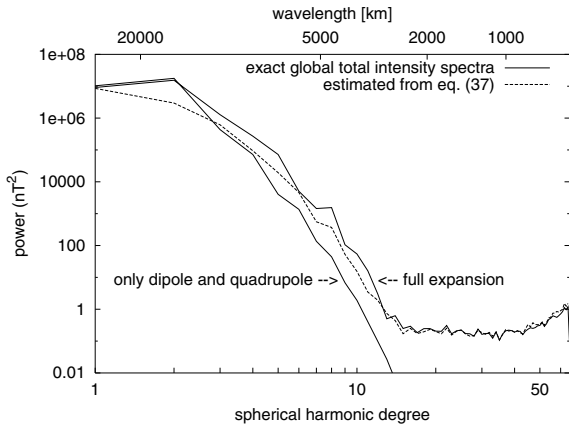
Figure 2. Verification of the total intensity spectrum estimated from Gauss coefficients: for the exact globally averaged total intensity spectrum, the total intensity on a latitude/longitude grid is computed from the spherical harmonic coefficients of the C89 global magnetic field model (Cain *et al.* 1989). A forward spherical harmonic transform gives the coefficients of the total intensity from which the total intensity spectrum is calculated using eq. (27). The dashed line indicates the spectrum estimated from the Gauss coefficients via eq. (42) using the globally averaged value of 5/12 for the term $(1 + \sin^2 I)/4$. The approximation holds well for the crustal part of the spectrum.

for the azimuthal average, while the second division by $(2\ell + 1)$ accounts for the Schmidt normalization. The solid line spectra in Fig. 2 were computed in this way.

Alternatively, the total intensity spectrum can be estimated directly from the Gauss coefficients as follows: Given the dominance of the main magnetic field, a high order magnetic field harmonic $\mathbf{B}_\ell^m$ contributes to the total intensity only with its component $\mathbf{B}_{\ell,m}^{\parallel}$ parallel to the main field. Hence, we have to derive an estimate of the expected power $E\{(\mathbf{B}_{\ell,m}^{\parallel})^2\}$.

Let us assume that the crustal magnetic field has stationary and isotropic statistical properties over the Earth's surface. Then the contribution of $\mathbf{B}_\ell^m$ to the power of the total intensity is

$$E\left\{\left(\mathbf{B}_{\ell,m}^{\parallel}\right)^2\right\} = E\left\{\left(\mathbf{b} \cdot \mathbf{B}_\ell^m\right)^2\right\} \tag{28}$$

$$= E\left\{\left(b_r B_{\ell,m}^r + \mathbf{b}_t \cdot \mathbf{B}_{\ell,m}^t\right)^2\right\}, \tag{29}$$

where $\mathbf{b}$ is a unit vector in the direction of the main field and the indices r and t denote the radial ($\parallel \mathbf{r}$) and tangential ($\perp \mathbf{r}$) parts of the vectors at the location $\mathbf{r}$. For this simple statistical model, the crustal field power depends only on the local inclination I of the main field. In this case, statistical expectation means that we have to average not only over all locations on the sphere, but also over all possible values of the main field declination δ as

$$E\left\{\left(\mathbf{B}_{\ell,m}^{\parallel}\right)^2\right\} = \left\langle \frac{1}{2\pi} \int_0^{2\pi} \left(b_r B_{\ell,m}^r + \mathbf{b}_t(\delta) \cdot \mathbf{B}_{\ell,m}^t\right)^2 d\delta \right\rangle \tag{30}$$

$$= \left\langle \left(b_r B_{\ell,m}^r\right)^2 + \underbrace{\frac{1}{\pi} \int_0^{2\pi} b_r B_{\ell,m}^r \mathbf{b}_t(\delta) \cdot \mathbf{B}_{\ell,m}^t d\delta}_{=0} \right.$$
$$\left. + \frac{1}{2\pi} \int_0^{2\pi} (\sin^2\delta \,(\mathbf{b}_t)^2 \left(\mathbf{B}_{\ell,m}^t\right)^2 d\delta \right\rangle \tag{31}$$

$$= b_r^2 \left\langle \left(B_{\ell,m}^r\right)^2 \right\rangle + \frac{1}{2}(\mathbf{b}_t)^2 \left\langle \left(\mathbf{B}_{\ell,m}^t\right)^2 \right\rangle \tag{32}$$

$$= \sin^2 I \left\langle \left(B_{\ell,m}^r\right)^2 \right\rangle + \frac{1}{2} \cos^2 I \left\langle \left(\mathbf{B}_{\ell,m}^t\right)^2 \right\rangle. \tag{33}$$

Here, the radial part $B_{\ell,m}^r$ and tangential part $\mathbf{B}_{\ell,m}^t$ of $\mathbf{B}_\ell^m$ are

$$B_{\ell,m}^r(r, \vartheta, \varphi) = (\ell + 1)\left(\frac{R_e}{r}\right)^{\ell+2} g_\ell^m \beta_\ell^m(\vartheta, \varphi) \tag{34}$$

$$\mathbf{B}_{\ell,m}^t(r, \vartheta, \varphi) = -\left(\frac{R_e}{r}\right)^{\ell+2} g_\ell^m \nabla_s \beta_\ell^m(\vartheta, \varphi), \tag{35}$$

where ∇_s and g_ℓ^m were defined above. From (34) and (35) the average strengths of the radial and tangential parts follow as (see Backus *et al.* 1996, p. 124, for a similar derivation):

$$\left\langle \left(B_{\ell,m}^r\right)^2 \right\rangle = (\ell + 1)^2 \left(\frac{R_e}{r}\right)^{2\ell+4} (g_\ell^m)^2 \left\langle (\beta_\ell^m)^2 \right\rangle \tag{36}$$

$$\left\langle \left(\mathbf{B}_{\ell,m}^t\right)^2 \right\rangle = \left(\frac{R_e}{r}\right)^{2\ell+4} (g_\ell^m)^2 \left\langle \nabla_s \beta_\ell^m \cdot \nabla_s \beta_\ell^m \right\rangle \tag{37}$$

$$= \left(\frac{R_e}{r}\right)^{2\ell+4} (g_\ell^m)^2 \left\langle -\beta_\ell^m \nabla_s^2 \beta_\ell^m \right\rangle \tag{38}$$

$$= \ell(\ell + 1)\left(\frac{R_e}{r}\right)^{2\ell+4} (g_\ell^m)^2 \left\langle (\beta_\ell^m)^2 \right\rangle. \tag{39}$$

For the high degree parts of the magnetic field $\langle B_r^2 \rangle / \langle (\mathbf{B}_t)^2 \rangle = (\ell + 1)/\ell \approx 1$, so their strength is half radial and half tangential (Holme & Jackson 1997). Thus, eq. (33) becomes

$$E\left\{\left(\mathbf{B}_{\ell,m}^{\parallel}\right)^2\right\} \approx \left(\frac{1}{2}\sin^2 I + \frac{1}{4}\cos^2 I\right) E\left\{\left(\mathbf{B}_\ell^m\right)^2\right\} \tag{40}$$

$$= \frac{1 + \sin^2 I}{4} E\left\{\left(\mathbf{B}_\ell^m\right)^2\right\}. \tag{41}$$

In particular, the ratio is 1/4 for equatorial and 1/2 for polar locations on the globe and its spherical average for a dipolar main field is 5/12. Superimposing a harmonic of degree ℓ onto a harmonic of degree 1 gives harmonics of degree $(\ell - 1)$ and $(\ell + 1)$. The precise relation (A5), derived in the Appendix, shows that the term of degree $(\ell - 1)$ dominates on average. Hence, $\mathbf{B}_\ell^{\parallel}$ contributes its power mainly to $|\mathbf{B}|_{\ell-1}$, rather than to $|\mathbf{B}|_\ell$. This is also mentioned without derivation by Arkani-Hamed *et al.* (1994). In summary, we obtain the relation

$$E\left\{|\mathbf{B}|_{\ell-1,m}^2\right\} \approx \frac{1 + \sin^2 I}{4} E\left\{\left(\mathbf{B}_\ell^m\right)^2\right\}, \quad \text{where } |m| < \ell. \tag{42}$$

However, relation (42) only holds if the decay of the true total intensity spectrum is less steep than the decay of the total intensity spectrum of the lower harmonics of the field. Otherwise, these lower harmonics dominate and (42) underestimates the true total intensity spectrum. This happens with the Earth's main field, as is illustrated in Fig. 2. For the crustal magnetic field, on the other hand, the relation appears to be quite accurate. Finally, note that relation (42) can be reversed. While the crustal magnetic vector field cannot be inferred unambiguously from total intensity data, we can get a reasonable estimate of its vector spectrum.

Plane power spectrum estimator

Apart from isolated Project Magnet aeromagnetic vector data, regional marine and aeromagnetic surveys usually provide only the total intensity of the field, denoted here by F. As before, we shall

write F as a sum of orthogonal contributions from decreasing wavelengths. For practical purposes, let an equidistant grid $F[x(i_1), y(i_2)]$ with side length L be given by the square Matrix $G(i_1, i_2)$, i_1, $i_2 = 0, \ldots, n - 1$. The matrix can be written as a discrete Fourier sum

$$G(i_1, i_2) = \frac{1}{n} \sum_{j_1=0}^{n-1} \sum_{j_2=0}^{n-1} \exp \frac{2\pi i(i_1 j_1 + i_2 j_2)}{n} \widetilde{G}(j_1, j_2), \qquad (43)$$

where $\widetilde{G}(j_1, j_2)$ is the discrete complex Fourier transform of $G(i_1, i_2)$ and j_1 and j_2 are integer indices. With definition (43) the Fourier transformed matrix fulfils

$$\sum_{i_1=0}^{n-1} \sum_{i_2=0}^{n-1} G(i_1, i_2)^2 = \sum_{j_1=0}^{n-1} \sum_{j_2=0}^{n-1} |\widetilde{G}(j_1, j_2)|^2. \qquad (44)$$

Indeed, it is recommended in the practical application of the following to check for this property, since fast Fourier transform (FFT) computer programs sometimes add factors of n and n^2 to either side of this equation. Since $G(i_1, i_2)$ is real valued, its complex Fourier transform $\widetilde{G}(j_1, j_2)$ has the property $\widetilde{G}(j_1, j_2) = \overline{\widetilde{G}(n - j_1, n - j_2)}$, $j_1, j_2 = 1, \ldots, n - 1$, where the bar denotes complex conjugation. Unfortunately, in this commonly used ordering of the grid $\widetilde{G}(j_1, j_2)$, the indices j_1 and j_2 do not directly reflect the overtone numbers (harmonics). To make it easier to implement the proposed equations in practice, let us introduce a re-arranged Fourier grid $\widetilde{G}'(j_1, j_2)$, where $j_1, j_2 = -n/2 + 1, \ldots, n/2$ are the harmonics of the grid:

$$\widetilde{G}'(j_1, j_2) = \widetilde{G}(j_1, j_2), \ 0 \leq j_1, \ j_2 \leq \frac{n}{2} \qquad (45)$$

$$\widetilde{G}'(-j_1, j_2) = \widetilde{G}(j_1, n - j_2), \ 0 \leq j_1 < \frac{n}{2}, \ 0 < j_2 \leq \frac{n}{2} \qquad (46)$$

$$\widetilde{G}'(j_1, -j_2) = \widetilde{G}(n - j_1, j_2), \ 0 < j_1 \leq \frac{n}{2}, \ 0 \leq j_2 < \frac{n}{2} \qquad (47)$$

$$\widetilde{G}'(-j_1, -j_2) = \widetilde{G}(n - j_1, n - j_2), \ 0 < j_1, \ j_2 < \frac{n}{2}. \qquad (48)$$

With this re-arranged grid, and using the estimate

$$\widehat{E}\{F[x(i_1), y(i_2)]^2\} = \frac{1}{n^2} \sum_{i_1=0}^{n-1} \sum_{i_2=0}^{n-1} G(i_1, i_2)^2, \qquad (49)$$

we can write eq. (44) as

$$\widehat{E}\{F[x(i_1), y(i_2)]^2\} = \frac{1}{n^2} \sum_{j_1, j_2=-n/2+1}^{n/2} |\widetilde{G}'(j_1, j_2)|^2. \qquad (50)$$

This is the plane counterpart to the discrete spherical harmonic representation of the estimated power in eq. (19). Similar to McKenzie's definition of an azimuthally summed plane spectrum for the gravity field (McKenzie 1994), we can define an azimuthal average $\overline{\widetilde{G}^2}(s)$ as a function of the harmonic $s = \sqrt{j_1^2 + j_2^2}$ as

$$\overline{\widetilde{G}^2}(s) = \frac{1}{n_s} \sum_{n_s} |\widetilde{G}'(j_1, j_2)|^2, \qquad (51)$$

where the sum extends over all index pairs (j_1, j_2) with $s - 0.5 \leq \sqrt{j_1^2 + j_2^2} < s + 0.5$. The number of such index pairs is denoted by n_s. With definition (51) as an azimuthal average, which is continuous in s, we can rewrite eq. (50) as

$$\widehat{E}\{F[x(i_1), y(i_2)]^2\} = \frac{1}{n^2} \int_0^\infty \overline{\widetilde{G}^2}(s)\, 2\pi s\, \mathrm{d}s. \qquad (52)$$

Finally, expressing the integrand in terms of the wavenumber $k = 2\pi s/L$ and substituting $\mathrm{d}s = L/2\pi\,\mathrm{d}k$ gives

$$\widehat{E}\{F[x(i_1), y(i_2)]^2\} = \int_0^\infty \underbrace{\frac{L^2}{(2\pi)^2\, n^2} \overline{\widetilde{G}^2}\left(\frac{Lk}{2\pi}\right)}_{T(k)} 2\pi k\, \mathrm{d}k \qquad (53)$$

with the total intensity spectral density

$$T(k) = \frac{L^2}{(2\pi)^2\, n^2} \overline{\widetilde{G}^2}\left(\frac{Lk}{2\pi}\right). \qquad (54)$$

Definition (54) is consistent with the azimuthally averaged power spectrum ('radial power spectrum') commonly used in applied gravity and magnetics, see for example, Spector & Grant (1970) or Blakely (1995, p. 415). Multiplication by $(L/n)^2$ makes the spectral density independent of the grid size and sampling interval. The division by $(2\pi)^2$ is necessary in order to fulfil condition (6), requesting that the integrated power spectral density be equal to the expected power. From (54) follows the discrete total intensity spectrum corresponding to (27) as

$$T_\ell = \frac{L^2}{4\pi\, R_e^2\, n^2} \overline{\widetilde{G}^2}\left[\frac{(2\ell + 1)L}{4\pi\, R_{\text{grid}}}\right], \qquad (55)$$

where the radial distance R_{grid} of the local grid from the Earth centre is likely to differ from the magnetic reference radius R_e.

Vector power spectrum estimated from plane total intensity data

Eq. (42) provides an estimate of the total intensity spectrum from the vector spectrum. We can now revert this relation and estimate the geomagnetic power spectrum at R_e from plane total intensity data. Using $k_{\ell+1} = k_\ell + 1/r$ we have

$$S_\ell \approx \left(\frac{R_{\text{grid}}}{R_e}\right)^{2\ell+4} \frac{4}{1 + \sin^2 I}\, T_{\ell+1} \qquad (56)$$

$$= \left(\frac{R_{\text{grid}}}{R_e}\right)^{2\ell+4} \frac{L^2}{\pi\,(1 + \sin^2 I)R_e^2\, n^2} \overline{\widetilde{G}^2}\left[\frac{(2\ell + 3)L}{4\pi\, R_{\text{grid}}}\right], \qquad (57)$$

where I is the inclination of the main magnetic field at the location of the grid.

APPLICATION

The main benefit of this precisely defined power spectrum is that it allows the comparison of spectra from different data sets, such as global models and grids of different side lengths and cell sizes. To illustrate the utility of the above derivations, the NGDC-720 spectrum is compared with local grids cut out of the NGDC World Magnetic Anomaly Map (WMAM) (Maus *et al.* 2007b).

Since NGDC-720 is a spherical harmonic model, the geomagnetic power spectrum can be inferred easily from its Gauss coefficients, using eq. (21). In contrast, estimation of the corresponding spectra from the regional grids requires a more complicated procedure.

(1) To obtain an approximately equal-area coverage of the spheroid with sample grids, a 20×20 mesh on the surface of a cube was projected onto the surface of the Earth. The mesh centres were then chosen as the centres of regional grids.

(2) For each grid location, a $20° \times 20°$ plane mesh with $0.05°$ cell spacing was projected onto the spheroid. For each cell, the total intensity anomaly was extracted from the WMAM grid. This corresponds to a projection of the WMAM onto local plane grids to avoid spherical distortion.

(3) For each grid, the spectrum was estimated by subtracting the mean, detrending, applying a sinusoidal taper, FFT, and azimuthal average.

(4) Taking into account the local inclination of the main field and the local difference between R_{grid} and R_e, the geomagnetic spectrum of each grid was estimated using eq. (57)

(5) Three averages of the grid spectra were computed: (1) an average of all grids, (2) an average of oceanic grids, defined as those having at least 90 per cent ocean coverage and (3) an average of continental grids, having not more than 40 per cent ocean coverage. A subsample of the grid outlines is displayed in Fig. 3. The same approach is also possible using single grids, but the power estimates at wavelengths close to the grid size then have high uncertainties. A large number of grids were, therefore averaged here, in order to obtain a precise estimate of the spectrum.

The resulting combined spectrum is displayed in Fig. 4. It shows excellent agreement of the average geomagnetic power spectrum estimate from plane data with the NGDC-720 spectrum. As expected, the field over continental crust is found to be stronger than over
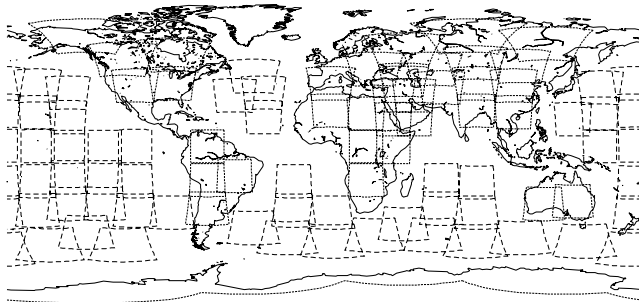

Figure 3. From 2400 plane grids, those with more than 90 per cent ocean coverage were chosen as ocean samples, and those with less than 40 per cent ocean coverage as land samples. Displayed here is only a small subset of the grids.
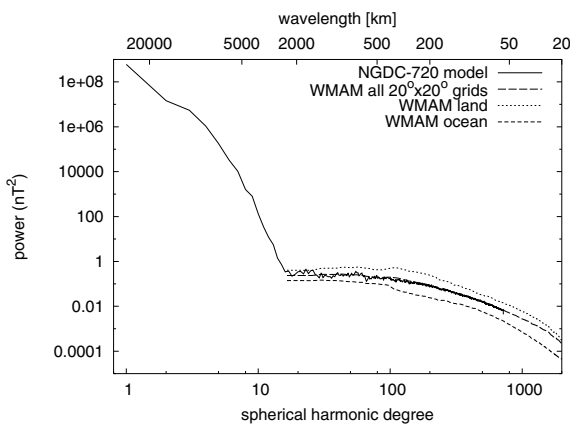

Figure 4. Geomagnetic power spectrum of NGDC-720 compared with the corresponding estimates from subgrids of NGDC's World Magnetic Anomaly Map. On average, magnetic anomalies over continental crust are significantly stronger than the global average, while anomalies over oceanic crust are usually weaker.

oceanic crust. This is likely due to differences in the thickness of the magnetized layer, but anomaly cancellation of adjacent stripes may also play a role in reducing the strength of the oceanic anomaly field.

The combined spectrum of Fig. 4 can also be used for identifying technical field modelling issues. The WMAM grid was produced by substituting the spherical harmonic coefficients of degrees 1–100 in the compilation of marine and aeromagnetic data with the corresponding coefficients of the satellite-based model MF5. The individual ocean and land averages show obvious steps at degree 100. A decrease in power in the ocean grids is explained by missing short wavelength signal (degree > 100) due to the limited marine data coverage in the southern oceans. The increase in the power over land at degree 100, on the other hand, could indicate missing signal in MF5 due to the filtering and line-levelling of the input satellite data, or it could indicate the presence of spurious anomalies in the continental compilations introduced by stitching together small, individual surveys. In the NGDC-720 spectrum, these differences average out, so that the model does not show any artefacts at degree 100. This illustrates the utility of comparing global and regional spectra for quality control in field modelling.

DISCUSSION AND CONCLUSIONS

The power spectrum is a valuable tool in many areas of science. In geomagnetism, the widespread use of degree variances as a geomagnetic power spectrum is a continuing source of confusion and misinterpretation. The fact that the degree variances are flat at the core–mantle boundary cannot be interpreted as a 'white depth' because degree variances slope upward for a spatially uncorrelated field. The long-wavelength crustal field, on the other hand, is indeed spatially uncorrelated at the Earth's surface, but this is obscured by upward sloping degree variances.

The geomagnetic power spectrum must be defined in such a way that it is flat for a spatially uncorrelated magnetic field. The definition proposed here retains the discrete nature of the degree variances and is displayed as a function of the spherical harmonic degree. To relate this global spectrum to spectra estimated from regional geomagnetic grids, one has to first derive the corresponding spectral density, which is a continuous function of the wavenumber. Via the spectral density, the high-degree part of the discrete geomagnetic power spectrum can be estimated from regional grids. A complication arises from the fact that local grids usually represent the anomaly of the total intensity. Hwoever as shown here, an accurate estimate of the geomagnetic power spectrum can de derived by considering that the total intensity anomaly is the projection of the anomaly vector onto the main field.

A comparison of the NGDC-720 geomagnetic power spectrum with corresponding estimates from regional subgrids of NGDC's World Magnetic Anomaly Map shows excellent agreement. This technique facilitates the identification of field modelling errors. It could also be used to compare the spectral content of different marine and aeromagnetic compilations. The ability to compare the global geomagnetic power spectrum with regional spectra provides a powerful aid in studying the influence of geological factors, such as crustal type and age, on magnetic anomaly strength. Dividing grids into oceanic and continental, it was shown here, for example, that magnetic anomalies are, on average, stronger over continental than over oceanic crust.

In merging the global geomagnetic spectrum with local spectra of regional grids, a consistent statistical interpretation of the Earth's internal magnetic field emerges: At short wavelengths (<50 km),

the spectrum falls off with a nearly constant slope in log–log scale. This is due to the self-similar (fractal) distribution of the crustal magnetization (Pilkington & Todoeschuck 1993; Maus & Dimri 1994). In the intermediate wavelength range (about 50–500 km) the curvature of the log–log spectrum follows naturally from the limited depth extent of the crustal magnetization, as can be reproduced from a slab model with self-similar magnetization (Maus *et al.* 1997). At longer wavelengths (500–2500 km) the spectrum is nearly flat, indicating that the crustal magnetic field is spatially uncorrelated. Finally, above wavelengths of 2500 km, the crustal field is masked by the main field from the Earth's core.

ACKNOWLEDGMENTS

REFERENCES

Arkani-Hamed, J., Langel, R.A. & Purucker, M., 1994. Scalar magnetic anomaly maps of Earth derived from POGO and Magsat data, *J. geophys. Res.*, **99,** 24 075–24 090.

Backus, G., Parker, R.L. & Constable, C., 1996. *Foundations of Geomagnetism,* Cambridge Univ. Press, Cambridge, UK.

Blakely, R.J., 1995. *Potential Theory in Gravity and Magnetic Applications,* Cambridge Univ. Press, Cambridge, UK.

Cain, J.C., Wang, Z., Kluth, C. & Schmitz, D.R., 1989. Derivation of a geomagnetic model to n = 63, *Geophys. J. Int.*, **97,** 431–441.

Hamoudi, M., Thebault, E., Lesur, V. & Mandea, M., 2007. Geoforschungszentrum anomaly magnetic map (gamma): a candidate model for the world digital magnetic anomaly map, *Geochem. Geophys. Geosyst.*, **8,** Q06023, doi:10.1029/2007GC001638.

Hemant, K., Thebault, E., Mandea, M., Ravat, D. & Maus, S., 2007. Magnetic anomaly map of the world: merging satellite, airborne, marine and ground-based magnetic data sets, *Earth planet. Sci. Lett.*, **260,** 56–71, doi:10.1016/j.epsl.2007.05.040.

Hipkin, R.G., 2001. The statistics of pink noise on a sphere: applications to mantle density anomalies, *Geophys. J. Int.*, **144,** 259–270.

Holme, R. & Jackson, A., 1997. The cause and treatment of attitude errors in near-Earth geomagnetic data, *Phys Earth planet. Inter.*, **103,** 375–388.

Jackson, A., 1996. Bounding the long-wavelength crustal magnetic field, *Phys. Earth planet. Int.*, **98,** 283–302.

Langel, R.A. & Estes, R.H., 1982. A geomagnetic field spectrum, *Geophys. Res. Lett.*, **9,** 250–253.

Lowes, F.J., 1966. Mean-square values on sphere of spherical harmonic vector fields, *J. geophys. Res.*, **71,** 2179.

Lowes, F.J., 1974. Spatial power spectrum of the main geomagnetic field, and extrapolation to the core, *Geophys. J. R. astr. Soc.*, **36,** 717–730.

Mauersberger, P., 1956. Das Mittel der Energiedichte des geomagnetischen Hauptfeldes an der Erdoberfläche und seine säkulare Änderung, *Gerlands Beitr. Geophys.*, **65,** 207–2015.

Maus, S. & Dimri, V.P., 1994. Scaling properties of potential fields due to scaling sources, *Geophys. Res. Lett.*, **21,** 891–894.

Maus, S., Gordon, D. & Fairhead, J.D., 1997. Curie-temperature depth estimation using a self-similar magnetization model, *Geophys. J. Int.*, **129,** 163–168.

Maus, S., Lühr, H., Rother, M., Hemant, K., Balasis, G., Ritter, P. & Stolle, C., 2007a. Fifth generation lithospheric magnetic field model from CHAMP satellite measurements, *Geochem. Geophys. Geosyst.*, **8,** Q05013, doi:10.1029/2006GC001521.

Maus, S., Sazonova, T., Hemant, K., Fairhead, J.D. & Ravat, D., 2007b. National geophysical data center candidate for the world digital magnetic anomaly map, *Geochem. Geophys. Geosyst.*, **8,** Q06017, doi:10.1029/2007GC001643.

McKenzie, D., 1994. The relationship between topography and gravity on Earth and Venus, *Icarus*, **112,** 55–88.

McLeod, M.G., 1996. Spatial and temporal power spectra of the geomagnetic field, *J. geophys. Res.*, **101,** 2745–2763.

McLeod, M.G. & Coleman, P.J., 1980. Spatial power spectra of the crustal geomagnetic field and core magnetic field, *Phys. Earth planet. Inter.*, **23,** P5–P19.

O'Brien, M.S., Parker, R.L. & Constable, C.G., 1999. Magnetic power spectrum of the ocean crust on large scales, *J. geophys. Res.*, **104,** 29 189–29 201.

Pilkington, M. & Todoeschuck, J.P., 1993. Fractal magnetization of continental crust, *Geophys. Res. Lett.*, **20,** 627–630.

Sabaka, T.J., Olsen, N. & Purucker, M.E., 2004. Extending comprehensive models of the Earth's magnetic field with Ørsted and CHAMP data, *Geophys. J. Int.*, **159,** 521–547.

Spector, A. & Grant, F.S., 1970. Statistical models for interpreting aeromagnetic data, *Geophysics*, **35,** 293–302.

Voorhies, C.V., Sabaka, T.J. & Purucker, M., 2002. On magnetic spectra of Earth and Mars, *J. geophys. Res. (Planets)*, **107,** doi:10.1029/2001JE001534.

APPENDIX A

In general, superimposing a harmonic of wavenumber ω_1 onto a harmonic of wavenumber ω_2 leads to a sum of harmonics with wavenumbers $(\omega_1 - \omega_2)$ and $(\omega_1 + \omega_2)$. Applied to the situation of an Earth with a dipolar main magnetic field of harmonic degree 1, a high degree harmonic $\mathbf{B}_\ell^m$ makes contributions of degrees $(\ell - 1)$ and $(\ell + 1)$ to the total intensity of the field. As shall be shown in the following, the contribution in terms of power to degree $(\ell - 1)$ is approximately one order of magnitude stronger than to degree $(\ell + 1)$, so the latter should be negligible in most cases.

Let us assume that the coordinate axis is aligned with the dipole axis. Then

$$\left|\mathbf{B}_{\ell,m}^{\|}\right| = \frac{\mathbf{B}_1^0 \cdot \mathbf{B}_\ell^m}{\left|\mathbf{B}_1^0\right|} = \frac{B_{1,0}^r B_{\ell,m}^r + \mathbf{B}_{1,0}^t \cdot \mathbf{B}_{\ell,m}^t}{\left|\mathbf{B}_1^0\right|}, \tag{A1}$$

where $\mathbf{B}_{\ell,m}^{\|}$ is the projection of $\mathbf{B}_\ell^m$ onto the direction of the main field. From eqs (34) and (35), with $\beta_1^0 \propto \cos\vartheta$ follows

$$\underbrace{\left[g_\ell^m\left(\frac{R_e}{r}\right)^{\ell+2}\right]^{-1}\sqrt{1 + 3\cos^2\vartheta}\,\left|\mathbf{B}_{\ell,m}^{\|}\right|}_{A_\ell^m}$$
$$= 2(\ell + 1)\cos\vartheta\,\beta_\ell^m - \sin\vartheta\,\partial_\vartheta\beta_\ell^m. \tag{A2}$$

To eliminate all occurrences of ϑ and ∂_ϑ, we require the following relations for fully normalized spherical harmonics

$$s^2\partial_\mu\beta_\ell^m = (\ell + 1)\mu\beta_\ell^m - \sqrt{\frac{(2\ell + 1)(\ell - m + 1)(\ell + m + 1)}{2\ell + 3}}\beta_{\ell+1}^m \tag{A3}$$

$$\mu\beta_\ell^m = \sqrt{\frac{(\ell - m)(\ell + m)}{(2\ell - 1)(2\ell + 1)}}\beta_{\ell-1}^m + \sqrt{\frac{(\ell - m + 1)(\ell + m + 1)}{(2\ell + 1)(2\ell + 3)}}\beta_{\ell+1}^m, \tag{A4}$$

where $s = \sin\vartheta$ and $\mu = \cos\vartheta$. Relations (A3) and (A4) are valid for all m and can be deduced from properties of the associated Legendre functions (Backus *et al.* 1996, eqs 3.7.38 and 3.7.14).

Using first (A3) and then (A4) in eq. (A2) gives

$$A_\ell^m = 3(\ell+1)\sqrt{\frac{(\ell-m)(\ell+m)}{(2\ell-1)(2\ell+1)}}\beta_{\ell-1}^m$$
$$+ (\ell+2)\sqrt{\frac{(\ell-m+1)(\ell+m+1)}{(2\ell+1)(2\ell+3)}}\beta_{\ell+1}^m. \qquad (A5)$$

Having used fully normalized spherical harmonics, we can argue that the first term on the right is three times stronger in amplitude, hence, roughly one order of magnitude stronger in power than the second term. However, this conclusion is valid only if the expectation for $(\mathbf{B}_\ell^\ell)^2$ and $(\mathbf{B}_\ell^{-\ell})^2$ is not higher than for the lower orders $|m| < \ell$.